

# Near-field optical spectroscopy of single quantum wires

T. D. Harris<sup>a)</sup>

*AT&T Bell Laboratories, 600 Mountain Ave. Murray Hill, New Jersey 07974*

D. Gershoni

*Department of Physics, Technion, Haifa 32000, Israel*

R. D. Grober

*Department of Applied Physics, Yale University, New Haven, Connecticut 06520-8284*

L. Pfeiffer, K. West, and N. Chand

*AT&T Bell Laboratories, Murray Hill, New Jersey 07974*

(Received 18 August 1995; accepted for publication 2 December 1995)

Low temperature near-field scanning optical microscopy is used for spectroscopic studies of single, nanometer dimension, cleaved edge overgrown quantum wires. A direct experimental comparison between a two dimensional system and a single genuinely one dimensional quantum wire system, inaccessible to conventional far field optical spectroscopy, is enabled by the enhanced spatial resolution. We show that the photoluminescence of a single quantum wire is easily distinguished from that of the surrounding quantum well. Emission from localized centers is shown to dominate the photoluminescence from both wires and wells at low temperatures. A factor of 3 absorption enhancement for these wires compared to the wells is concluded from the photoluminescence excitation data. © 1996 American Institute of Physics. [S0003-6951(96)04406-1]

Optoelectronics based on very thin layers of semiconductor heterostructures, such as quantum wells (QWs), are now dominant for many commercial applications. In an attempt to gain further from the reduction of dimensionality,<sup>1</sup> a world wide research effort to bring 1D quantum structures such as quantum wires (QWRs) and 0D quantum structures such as quantum dots to the same degree of perfection achieved in the 2D quantum systems has been underway during the last decade.

Among the most promising ways to achieve this goal for 1D structures is cleaved edge overgrowth (CEO).<sup>2</sup> This technique utilizes two orthogonal directions of epitaxial growth, exploiting the precision of layer thickness control to form uniform intersecting planes of semiconductor. Two different CEO quantum wire systems have been fabricated and studied: (a) Strained layer QWRs (SQWRs) in which confinement to 1D is produced by one dimensional pseudomorphic strain induced in the (110) oriented cleaved edge QW by a (100) oriented strained layer QW.<sup>3</sup> (b) T-shaped QWRs (TQWRs) in which quantum confinement to 1D is produced along the intersection line between the planes of a (100) oriented QW and that of a (110) oriented cleaved edge overgrown QW.<sup>4</sup>

Study of single CEO-QWRs requires care to ensure the unambiguous separation of wire and well spectroscopy. Far field optical spectroscopy has proved to be the most revealing tool for the characterization of 2D structures<sup>5</sup> but suffers a substantial obstacle for CEO QWRs. The probed volume of QW is orders of magnitude larger than the probed volume of a QWR. The QWR spectral features are likely obscured by or attributed to QW features. We show here that the enhanced spatial resolution of low temperature near-field scanning optical microscopy (LT-NSOM) surmounts this obstacle, permitting unambiguous single QWR studies. There is substantial existing spectroscopic data on multiple and arrays

of CEO QWRs.<sup>3,4,6-8</sup> The added clarity of probing a single wire structure is considerable, since heterogeneity and carrier and electromagnetic field interactions between neighboring wires are eliminated. We report here low temperature, near field imaging spectroscopy of the first CEO system, SQWRs.

The low temperature NSOM microscope used for this study has been described in detail.<sup>9</sup> Different from this prior report, all the data reported here used excitation and collection with the same aluminum coated, tapered fiber probe at a sample temperature of 4 K. The excitation radiation was launched to the fiber from a computer controlled Ti:sapphire laser. An intensity stabilizer ("noise eater") and quarter- and half-wave plates were inserted between two separate sections of the Corning 850 nm single mode fiber used for our NSOM probes. Fusion spliced into the second section of the fiber is a 3 dB two way splitter. It provides a convenient means of simultaneously monitoring the light sent to the probe, and detecting the light collected by the probe. In order to simultaneously excite and detect through the same tip, efficient discrimination between excitation and emitted light is required. Elastically scattered light is efficiently filtered by a triple spectrometer. The fiber used in this study had no significant fiber fluorescence for the relevant excitation wavelengths (700–800 nm). We thus attribute the background light detected to either fluorescence from the aluminum silica interface or to Raman scattering within the fiber itself. This background light is typically 1–2 orders of magnitude larger than the photoluminescence (PL) signal collected by the tip (diameter > 200 nm), highly structured, and strongly polarized parallel to the exciting radiation. By careful adjustment of retardation plates in both the excitation and detection channels, extinction ratios of sample luminescence to background of as much as 3 orders of magnitude could be achieved. The light emitted around the fiber tip was collected by a reflecting objective contained within the cryostat and directed to a second CCD camera equipped monochromator.

The sample studied here was grown as follows. In the

<sup>a)</sup>Electronic mail: tdh@clockwise.att.com

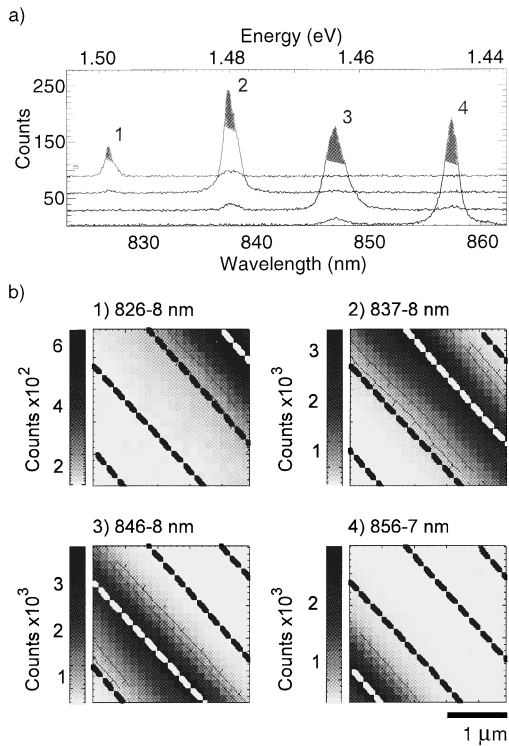


FIG. 1. (a) Single pixel PL spectra from an NSOM image. If the emission intensity is integrated over the shaded wavelength interval, the (b) four fixed wavelength emission images result. Images are numbered from the spectra indicating the wavelength interval.

first growth step, molecular beam epitaxy (MBE) was used to grow five strained  $\text{In}_{0.10}\text{Ga}_{0.90}\text{As}$  QWs of 300, 150, 75, 38, and 18 Å respectively, on a (100) oriented GaAs substrate. The strained QWs, are separated by 1.0 μm thick layers of GaAs and capped by a 2 μm thick GaAs layer. It was cleaved during growth, exposing a (110) facet onto which the following layers were grown in succession: 200 Å  $\text{Al}_{0.3}\text{Ga}_{0.7}\text{As}$ , 80 Å GaAs, 200 Å  $\text{Al}_{0.3}\text{Ga}_{0.7}\text{As}$ , 35 Å GaAs, 200 Å  $\text{Al}_{0.3}\text{Ga}_{0.7}\text{As}$ , and 50 Å GaAs. On the cleaved face are thus formed ten single SQWRs, one wire in each of two (110) QWs, for each of the five (100) strained InGaAs QWs. Low temperature cathodoluminescence (CL) was used previously to show that emission from the AlGaAs/GaAs (110) QWs is red shifted directly above the strained layers.<sup>8,10</sup> Here, using NSOM spectroscopy we overcome two major disadvantages of CL: (a) The loss of spatial resolution due to the large diffusion length ( $\sim 1 \mu\text{m}$ ) of the high excess energy cathodo-excited carriers. (b) The lack of excitation energy tunability.

Two modes of data acquisition were used: PL spectral images are generated by fixing the excitation energy and recording a PL spectrum for 1–5 s at each tip position. A large four dimensional ( $x, y, \lambda, I$ ) data set is thus generated. Alternately, at a single tip position (image pixel  $-x, y$ ), emission intensity integrated over a selected spectral range is recorded as a function of the excitation energy.

In Fig. 1(a) we show four PL spectra which were selected from the 441 near-field spectra generated in a  $21 \times 21$  pixel scan of a  $2.5 \times 2.5 \mu\text{m}$  square region of the CEO SQWR sample. The spectra are vertically displaced for clar-

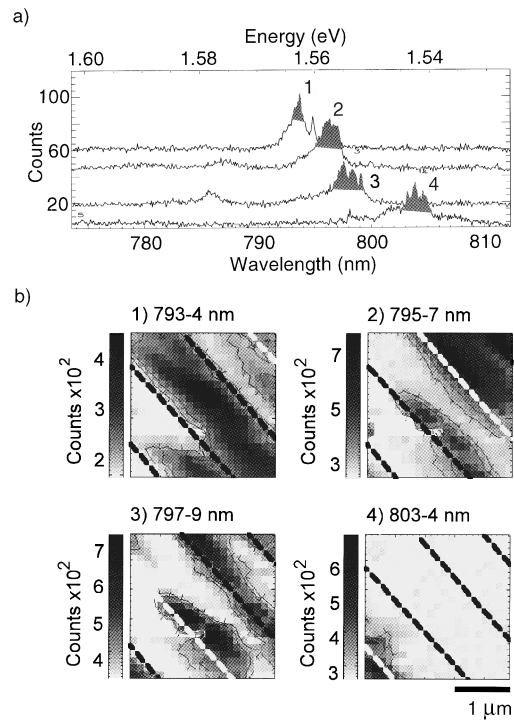


FIG. 2. (a) Single pixel PL spectra from the same area as Fig. 2(b) for wavelength near the 80 Å (110) QW. (b) Fixed wavelength images for the shaded intervals shown above.

ity. In each spectrum a distinct spectral line is observed. These lines arise from carrier recombination within the (100) oriented strained InGaAs QWs. The spectrum marked “1” results from recombination in the 18 Å strained QW and the lines marked “2,” “3,” and “4” result from recombination within the 38, 75 and 150 Å strained QWs, respectively. In Fig. 1(b) we show the four selective wavelength PL images associated with the spectral lines of Fig. 1(a). The images are obtained by integrating the PL emission over the wavelength interval marked in gray on Fig. 1(a). These images allow an accurate determination of the spatial source for each spectral feature. The position of the (100) oriented strained 18, 38, 75 and 150 Å InGaAs QWs is clearly identified by these images. We have marked these positions by the bold dash lines on the images, for later reference.

In Figs. 2(a) and 2(b) we show PL spectra and fixed wavelength images for recombination associated with the 80 Å (110) oriented GaAs/AlGaAs QW for the same scan area as for Fig. 1. The four dashed bold lines of Fig. 2(b) mark the position of the strained (100) oriented InGaAs QWs as determined from Fig. 1(b). The upper most spectrum in Fig. 2(a), marked “1,” is dominated by a spectral feature which peaks at 793 nm. This PL emission line is typical of the (110) oriented CEO 80 Å GaAs/AlGaAs QW as verified by far field spectroscopy in this work and previous studies.<sup>3,7,8</sup> Spectrum “1” is from a pixel midway between the 38 Å and 75 Å strained QW. The image clearly shows that the spatial origin of this emission strongly anticorrelates with the positions of the strained QWs. The lower three spectra in Fig. 2(a), marked “2,” “3,” and “4,” originate from pixels above 3 of the strained QWs. The fixed wavelength images of these spectral lines strongly correlate with the spatial position of

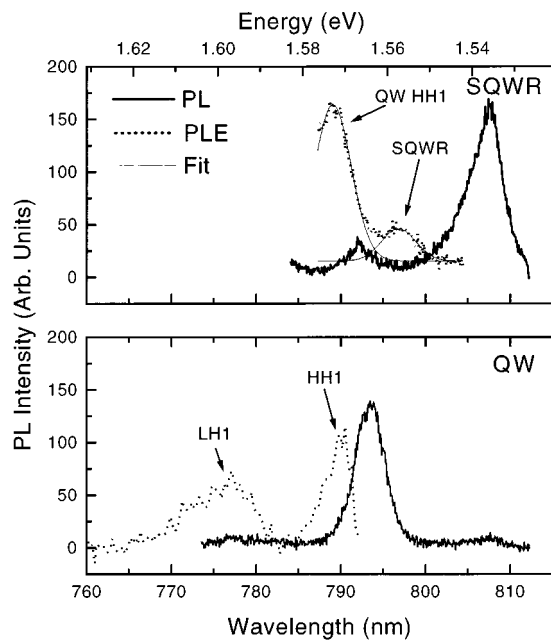


FIG. 3. Near-field PL (solid line) and PLE (dotted line) spectra of the 80 Å (110) QW (lower panel) and the 150 Å × 80 Å SQWR (upper panel). A two Gaussians model fit used to determine the relative intensity is shown by the thin solid line.

the (100) oriented strained InGaAs QWs, as can be seen in Fig. 2(b). The three lower PL spectra in Fig. 2(a) are thus assigned to carrier recombination within the single SQWRs. The magnitude of these shifts is in agreement with previous measurements using far field optics and a large array of QWRs.<sup>3,7,8</sup> We note that both the PL images and the near-field PL spectra (sharp spectral “spikes”) clearly indicate that the emission from both the QWs and QWRs originate from fully (0D) localized centers.<sup>11</sup>

In Fig. 3 we show the PL (solid line) and PLE (dotted line) spectra of the 150 Å SQWR and the (110) oriented 80 Å GaAs QW from a position between the strained (100) oriented InGaAs QWs. The all near-field PLE spectrum of the (110) CEO GaAs QW is indistinguishable from the far field PLE spectrum (not shown). The excitonic transitions associated with the first heavy-hole excitons (HH1) and the first light-hole exciton (LH1) are marked in Fig. 3. The 5 meV Stokes shift between the HH1 transition measured in PLE and that measured in PL is typical of (110) oriented QWs.<sup>12</sup> Since the NSOM tip, 3000 Å diameter is far larger than the SQWR, excitation of carriers in the QW can not be avoided. If there is efficient carrier diffusion, the spectral features associated with QW absorption are seen in the PLE spectrum of the SQWR. The spectral feature centered at 799 nm in the PLE spectrum of the SQWR is at a lower energy than the QW band edge and thus can only be assigned to SQWR absorption. With a few reasonable assumptions, the data of Fig. 3 can be used to experimentally test the prediction of enhanced absorption for QWR structures.<sup>1</sup> We assume that all photogenerated carriers up to a tip radius diffuse to recombine in the SQWR. This assumption is supported by the spectra and images of Fig. 2. There is negligible emission from the QW when the tip is positioned directly over a QWR. Variation of carrier localization with

position causes the selective wavelength images of Fig. 2 to appear “blotchy.” Integration of all emission at any image pixel shows uniform PL efficiency. Since the magnitudes of PL emission from the SQWRs and the QW are comparable, nonradiative recombination can be reasonably ignored. Thus the ratio of QW and QWR absorption strength can be measured by comparing the peak area of the lowest energy transition of the QW to that of the SQWR as observed in the PLE spectrum of the SQWR, correcting for the geometric area of the two structures. The QW to SQWR area ratio under the tip is approximately 20:1, while the QW-QWR PLE intensity ratio is roughly 6:1 as determined by the two Gaussians model fit to the data shown in Fig. 3. A factor of 3 enhancement in the absorption of the wire with respect to that of the well is thus determined. This measured increase in the QWR absorption strength is in agreement with theoretical estimations.<sup>13</sup> The data of Fig. 3 are the best signal to noise obtained in many attempts. A systematic study of absorption enhancement with wire width and variation with position on each wire are required to confirm this preliminary result.

Using NSOM spectroscopy, we produce photoluminescence and photoluminescence excitation spectra of single quantum wires. The spatial position of strained, cleaved edge overgrown (110) quantum wires is coincident with the underlying strained (100) quantum wells, and the magnitude of the SQWR energy shift scales with this (100) QW width. From the near-field PLE spectrum we estimate a factor of three absorption strength enhancement for this semiconductor quantum wire relative to a comparable QW.

- <sup>1</sup> Y. Arakawa and H. Sakaki, *Appl. Phys. Lett.* **40**, 939 (1982); Y. Arakawa, K. Vahala, and A. Yariv, *Appl. Phys. Lett.* **45**, 950 (1984).
- <sup>2</sup> L. N. Pfeiffer, K. W. West, H. L. Stormer, J. Eisenstein, K. W. Baldwin, D. Gershoni, and J. Spector, *Appl. Phys. Lett.* **56**, 1697 (1990).
- <sup>3</sup> D. Gershoni, J. S. Weiner, S. N. G. Chu, G. A. Baraff, J. M. Vandenberg, L. N. Pfeiffer, K. W. West, R. A. Logan, and T. Tanbun-Ek, *Phys. Rev. Lett.* **65**, 1631 (1990).
- <sup>4</sup> A. R. Goni, L. N. Pfeiffer, K. W. West, A. Pinczuk, H. U. Baranger, and H. L. Stormer, *Appl. Phys. Lett.* **61**, 1956 (1992).
- <sup>5</sup> R. Dingle, W. Wiegmann, and C. H. Henry, *Phys. Rev. Lett.* **33**, 827 (1974).
- <sup>6</sup> W. Wegscheider, L. N. Pfeiffer, M. M. Dignam, A. Pinczuk, K. W. West, S. L. McCall, and R. Hull, *Phys. Rev. Lett.* **71**, 4071 (1993).
- <sup>7</sup> D. Gershoni, M. Katz, W. Wegscheider, L. N. Pfeiffer, R. A. Logan, and K. W. West, *Phys. Rev. B* **50**, 8930 (1994).
- <sup>8</sup> D. Gershoni, J. S. Weiner, E. A. Fitzgerald, L. N. Pfeiffer, and N. Chand, in *Optical Phenomena in Semiconductor Structures of Reduced Dimensions*, edited by D. J. Lockwood and A. Pinczuk (Kluwer, Dordrecht, 1993), p. 337.
- <sup>9</sup> R. D. Grober, T. D. Harris, J. K. Trautman, and E. Betzig, *Rev. Sci. Instrum.* **65**, 626 (1994).
- <sup>10</sup> D. Gershoni, J. S. Weiner, S. N. G. Chu, G. A. Baraff, J. M. Vandenberg, L. N. Pfeiffer, K. West, R. A. Logan, and T. Tanbun-Ek, *Phys. Rev. Lett.* **66**, 1375 (1991).
- <sup>11</sup> H. F. Hess, E. Betzig, T. D. Harris, L. N. Pfeiffer, and K. W. West, *Science* **264**, 1740 (1994).
- <sup>12</sup> D. Gershoni, I. Brener, G. A. Baraff, S. N. G. Chu, L. N. Pfeiffer, and K. West, *Phys. Rev. B* **44**, 1931 (1991).
- <sup>13</sup> I. Suemune and L. A. Coldren, *IEEE J. Quantum Electron.* **24**, 1778 (1988).